Behavioral/Systems/Cognitive

Nonthermal Activation of Transient Receptor Potential Vanilloid-1 Channels in Abdominal Viscera Tonically Inhibits Autonomic Cold-Defense Effectors

Alexandre A. Steiner,[1] Victoria F. Turek,[1] Maria C. Almeida,[1] Jeffrey J. Burmeister,[1] Daniela L. Oliveira,[1] Jennifer L. Roberts,[1] Anthony W. Bannon,[2] Mark H. Norman,[3] Jean-Claude Louis,[2] James J. S. Treanor,[2] Narender R. Gavva,[2] and Andrej A. Romanovsky[1]

[1]Systemic Inflammation Laboratory, Trauma Research, St. Joseph's Hospital, Phoenix, Arizona 85013, and Departments of [2]Neuroscience and [3]Chemistry Research and Discovery, Amgen, Thousand Oaks, California 91320

An involvement of the transient receptor potential vanilloid (TRPV) 1 channel in the regulation of body temperature (T_b) has not been established decisively. To provide decisive evidence for such an involvement and determine its mechanisms were the aims of the present study. We synthesized a new TRPV1 antagonist, AMG0347 [(*E*)-*N*-(7-hydroxy-5,6,7,8-tetrahydronaphthalen-1-yl)-3-(2-(piperidin-1-yl)-6-(trifluoromethyl)pyridin-3-yl)acrylamide], and characterized it *in vitro*. We then found that this drug is the most potent TRPV1 antagonist known to increase T_b of rats and mice and showed (by using knock-out mice) that the entire hyperthermic effect of AMG0347 is TRPV1 dependent. AMG0347-induced hyperthermia was brought about by one or both of the two major autonomic cold-defense effector mechanisms (tail-skin vasoconstriction and/or thermogenesis), but it did not involve warmth-seeking behavior. The magnitude of the hyperthermic response depended on neither T_b nor tail-skin temperature at the time of AMG0347 administration, thus indicating that AMG0347-induced hyperthermia results from blockade of tonic TRPV1 activation by nonthermal factors. AMG0347 was no more effective in causing hyperthermia when administered into the brain (intracerebroventricularly) or spinal cord (intrathecally) than when given systemically (intravenously), which indicates a peripheral site of action. We then established that localized intra-abdominal desensitization of TRPV1 channels with intraperitoneal resiniferatoxin blocks the T_b response to systemic AMG0347; the extent of desensitization was determined by using a comprehensive battery of functional tests. We conclude that tonic activation of TRPV1 channels in the abdominal viscera by yet unidentified nonthermal factors inhibits skin vasoconstriction and thermogenesis, thus having a suppressive effect on T_b.

Key words: TRPV1; channel; chemosensory; afferent; temperature; hyperthermia

Introduction

The transient receptor potential vanilloid (TRPV) 1 channel is abundant in small-diameter sensory fibers of spinal and cranial nerves, as well as in several populations of neurons within the CNS (Tominaga and Caterina, 2004; Dhaka et al., 2006). The TRPV1 channel, one of the so-called ThermoTRP channels, is activated with a high gain by heat, protons, and vanilloids; acti-

vation (opening) of this channel results in an inward nonselective cationic current that promotes both cell depolarization and an upsurge of cytosolic calcium (Caterina et al., 1997; Tominaga et al., 1998). In transfected cells maintained at a physiological pH (7.4), the threshold temperature for activation of the TRPV1 channel is ∼43°C (Caterina et al., 1997; Tominaga et al., 1998). Hence, this channel was anticipated to contribute to the detection of noxious temperatures but not to physiological thermoregulation. A role of the TRPV1 channel in thermal nociception has been confirmed by studies with genetic deletion (Caterina et al., 2000; Davis et al., 2000) or pharmacological blockade (Garcia-Martinez et al., 2002; Gavva et al., 2005b) of this channel. The noninvolvement of the TRPV1 channel in the physiological regulation of deep body temperature (T_b) has been accepted based on the fact that TRPV1-deficient mice regulate T_b similarly to wild-type mice when exposed to various thermal environments (Szelenyi et al., 2004; Iida et al., 2005). Most recently, the idea that the TRPV1 channel does not play a role in T_b regulation has been challenged by the observation that some drugs that block the TRPV1 channel can increase T_b of rats, dogs, and monkeys (Swanson et al., 2005; Gavva et al., 2007). However, it has not

been proven definitively whether the hyperthermic effects of these drugs are attributable to the blockade of the TRPV1 channel or to a yet unidentified side action.

In the present study, we synthesized a new TRPV1 antagonist, AMG0347 [(E)-N-(7-hydroxy-5,6,7,8-tetrahydronaphthalen-1-yl)-3-(2-(piperidin-1-yl)-6-(trifluoromethyl)pyridin-3-yl)acrylamide], and characterized it in vitro. We then showed that AMG0347 is the most potent TRPV1 antagonist known to cause hyperthermia in rats and mice and that its effect on T_b occurs through the TRPV1 channel. As of today, these data provide the strongest evidence of a tonic involvement of the TRPV1 channel in thermoregulation. We then identified the mechanisms of AMG0347-induced hyperthermia.

Materials and Methods

Synthesis of AMG0347
AMG0347 (for chemical structure, see Fig. 1A) was synthesized as described in supplemental Materials and Methods (available at www.jneurosci.org as supplemental material).

In vitro $^{45}Ca^{2+}$ uptake assays
Chinese hamster ovary cells stably transfected with the rat or human TRPV1 channel (Gavva et al., 2004, 2005b) were seeded in the wells (20,000 cells per well) of a Cytostar 96-well plate (GE Healthcare, Little Chalftont, UK). Two days later, the assays were conducted. For assessment of the ability of AMG0347 or AMG9810 [(E)-3-(4-t-butylphenyl)-N-(2,3-dihydrobenzo[1,4]dioxin-6-yl)acrylamide] to block TRPV1 channel activation by capsaicin, the cells were incubated for 2 min at room temperature with capsaicin (500 nM) and one of the antagonists (20 pM to 4 μM) in HBSS, pH 7.4, supplemented with bovine serum albumin (100 μg/ml) and HEPES (1 mM). $^{45}Ca^{2+}$ (MP Biomedicals, Irvine, CA) in Ham's F-12 medium was then added to achieve a final concentration of 10 μCi/ml, and the cells were incubated for additional 2 min at room temperature. At the end of the second incubation, the wells containing the cells were thoroughly washed with PBS (10 μM; pH 7.4) containing bovine serum albumin (100 μg/ml). The amount of $^{45}Ca^{2+}$ in the cells was measured using a scintillation counter (MicroBeta Jet; PerkinElmer, Wellesley, MA). For assessment of the effects of the antagonists on TRPV1 channel activation by heat, the assay was performed as before, except that capsaicin was not present during the first incubation and that the second incubation was conducted at 45°C in a dry bath incubator (PH-100; Boekel Scientific, Feasterville, PA). For assessment of the effects of the antagonists on TRPV1 channel activation by protons, the cells were initially incubated for 2 min at room temperature with AMG0347 or AMG9810 in an acid buffer (MES buffer, pH 5) supplemented with HEPES (30 mM), after which the assay proceeded as described above for the activation by capsaicin assay.

Animals
The experiments were conducted in rats and mice under protocols approved by the St. Joseph's Hospital Animal Care and Use Committee. Male Wistar rats were obtained from Harlan (Indianapolis, IN). They were housed in cages kept in a rack equipped with a Smart Bio-Pack ventilation system and Thermo-Pak temperature control system (Allentown Caging Equipment, Allentown, NJ); the temperature of the incoming air was maintained at 28°C. Standard rat chow and tap water were available ad libitum. The room was on a 12 h light/dark cycle (lights on at 7:00 A.M.). Each rat was extensively handled and habituated to staying inside wire-mesh conical confiners (used later in the thermocouple-respirometry setup) or in the channels of the thermogradient apparatus (thermogradient setup). At the time of the experiments, the rats weighed 300–450 g.

Mice with ($^{-/-}$) or without ($^{+/+}$) a homozygous targeted null mutation in the TRPV1 gene (Caterina et al., 2000) were obtained from the Amgen colony at Charles River Laboratories (Wilmington, MA). They were housed in cages kept in a Maxi-Miser ventilated rack (Thoren Caging Systems, Hazleton, PA) at an ambient temperature (T_a) of 27°C. Standard mouse chow and tap water were available ad libitum. The room

was on a 12 h light/dark cycle (lights on at 7:00 A.M.). Each mouse was extensively handled and habituated to spending time inside a Plexiglas enclosure as described previously (Rudaya et al., 2005); the same enclosures were used later in experiments (telemetry setup). At the time of the experiments, the mice weighed 30–40 g.

Surgical preparations
Each rat or mouse was subjected to one or more of the surgical procedures described below. All procedures were performed 5–7 d before an experiment, except for the arterial catheterization (which was performed 1–2 d before an experiment).

Anesthesia and perioperative care. Immediately after anesthesia was induced by intraperitoneal ketamine–xylazine–acepromazine (55.6, 5.5, and 1.1 mg/kg for rats; 42.0, 4.8, and 0.6 mg/kg for mice), the animals were treated prophylactically with an antibiotic (enrofloxacin, 1.1 mg/kg, s.c.). During surgery, the animals were kept on a heating pad; mice were periodically (every 5 min) ventilated with oxygen through custom-made masks. To prevent postsurgical hypothermia, the animals were allowed to recover from anesthesia in a climatic chamber set to 28°C (rats) or 31°C (mice).

Implantation of temperature-measuring devices. A mouse designated for an experiment in the telemetry setup was implanted with a miniature telemetry transmitter (G2 E-Mitter series; Mini Mitter, Bend, OR), whereas a rat designated for an experiment in the thermogradient setup was implanted with a miniature temperature datalogger (SubCue, Calgary, Alberta, Canada). The devices were implanted into the peritoneal cavity via a midline laparotomy and then fixed to the lateral abdominal wall with sutures. The abdominal muscles and skin were sutured in layers.

Intraperitoneal catheterization. This procedure was performed in mice only. After a small midline incision, a silicone catheter [inner diameter (ID), 0.5 mm; outer diameter (OD), 0.9 mm] filled with pyrogen-free saline was inserted into the peritoneal cavity and fixed in place by being sutured to the abdominal wall. The free end of the catheter was knotted, tunneled under the skin to the nape, and exteriorized. The abdominal surgical wound was sutured. The catheter was flushed with saline on the day after surgery and every other day thereafter.

Intravenous catheterization. This and all other procedures described below were performed in rats only. A small longitudinal incision was made on the ventral surface of the neck, left of the trachea. The left jugular vein was exposed, freed from its surrounding connective tissue, and ligated. A silicone catheter (ID, 0.5 mm; OD, 0.9 mm) filled with heparinized (10 U/ml) saline was passed into the superior vena cava through the jugular vein and secured in place with ligatures. The free end of the catheter was knotted, tunneled under the skin to the nape, and exteriorized. The skin wound was sutured. The catheter was flushed with heparinized saline the day after surgery and every other day thereafter.

Arterial catheterization. The neck was incised as for the venous catheterization, and the right carotid artery was isolated and clamped by a microclip. A polyethylene (PE)-50 catheter (ID, 0.6 mm; OD, 1.0 mm) filled with heparinized saline was inserted into the artery toward the heart, the clip was removed, and the catheter was secured in place with ligatures. The free end of the catheter was heat closed and exteriorized at the nape. The surgical wound was sutured.

Intracerebroventricular cannulation. A rat was fixed to a stereotaxic apparatus (David Kopf Instruments, Tujunga, CA) with the incisor bar set 3.3 mm ventral to interaural line. The skin was incised over the sagittal suture, the periosteum was excised, four supporting microscrews were driven into the skull, and a steel guide cannula (Plastics One, Roanoke, VA) was implanted. The tip of the cannula was placed just dorsal to the right lateral ventricle (−0.8 mm from bregma, −1.5 mm from the midline, and 2.5 mm from the skull surface) or the third ventricle (0.0 mm from bregma, 0.0 mm from the midline, and 6.0 mm from the skull surface). The implanted cannula was attached to the microscrews with acrylic cement. The lateral ventricle cannula was used to deliver AMG0347 (or vehicle) in experiments designed to compare different routes of administration (supplemental Fig. 2, available at www.jneurosci.org as supplemental material); the third ventricle cannula was used to deliver capsaicin for the centrally induced vasodilation test (see Fig. 5).

Intrathecal catheterization. This procedure was performed as detailed previously (Pogatzki et al., 2000). Briefly, a rat was placed in a kyphotic position, and the skin on the back was incised along the midline at the level of the iliac crests. The space between lumbar vertebrae 5 and 6 was punctured with a 23 gauge hypodermic needle, which was pushed in until it reached the thecal space; penetration into the thecal space was associated with a tail-flick or hind-paw retraction. A 32 gauge polyurethane catheter reinforced with a steel stylet (Micor, Allison Park, PA) was passed through the needle into the thecal space and advanced rostrally by 4.0 cm from the surface of the body. The stylet and the needle were then removed, and the exterior end of the catheter was bound to a PE-50 catheter using Scotch-Weld structural plastic adhesive (DP-8010; 3M, St. Paul, MN). After the adhesive cured for 20 min, the extended catheter was filled with saline, and its free end was heat closed and exteriorized at the nape. The incised skin was sutured.

Experimental setups
Three setups were used.

Telemetry setup. Telemetry receivers (model ER-4000; Mini Mitter) were positioned inside a climatic chamber (model 3940; Forma Scientific, Marietta, OH). The home cage of each mouse was placed on top of a receiver, a Plexiglas enclosure was placed inside the cage, and the mouse was left in the enclosure. If the mouse had been preimplanted with a catheter for drug administration, a PE-50 catheter extension was passed through a wall port of the climatic chamber and connected to a syringe. In this setup, T_a values of 31°C and 26°C are neutral and subneutral, respectively, for mice (Rudaya et al., 2005).

Thermocouple-respirometry setup. Rats were placed in confiners and equipped with copper-constantan thermocouples for recording colonic temperature and tail-skin temperature (T_{sk}). The thermocouples were plugged into a data logger (Cole-Parmer, Vernon Hills, IL). Each rat in the confiner was then placed inside a cylindrical Plexiglas chamber (Sable Systems, Las Vegas, NV), which was sealed and continuously ventilated; the airflow was maintained at 600 ml/min with the help of a mass flow controller (Sierra Instruments, Monterey, CA). The air leaving each chamber was automatically sampled, dried, and passed thought an oxygen analyzer (Sable Systems). The Plexiglas chamber containing the rat was kept inside a climatic chamber (Forma Scientific). When present, a catheter (venous, arterial, or thecal) was connected to a PE-50 extension filled with saline. When the animal had an intracerebroventricular cannula, a needle injector was fitted into the cannula and connected to a PE-50 extension. The extension (from the catheter or intracerebroventricular injector) was passed through a port of the Plexiglas chamber, and the port was sealed with paraffin. The extension was then passed through a port of the climatic chamber and connected to a syringe. Using a method previously developed in our laboratory (Romanovsky et al., 2002), we found that T_a values of 23–29°C were neutral for rats in this setup.

Thermogradient setup. The six-channel thermogradient apparatus used has been described in detail previously (Almeida et al., 2006b). Each rat was allowed to move freely inside a long aluminum channel that had a linear T_a gradient (15–30°C). To make an injection in the thermogradient setup, Plexiglas barriers were used to briefly confine the rat to the same portion of the 200-cm-long channel that it was selecting immediately before the injection; after the drug was injected through the jugular catheter, the barriers were removed.

Drug administration
In thermophysiology experiments, AMG0347 and resiniferatoxin (RTX) were administered to rats and mice as described below.

Intraperitoneal AMG0347 to mice. Aliquots of an ethanolic stock solution of AMG0347 (3.5 mg/ml) were stored at −80°C. On the day of the experiment, the stock was diluted with ethanol and saline to give a working solution of AMG0347 (15 or 150 µg/ml) in 50% ethanol. AMG0347 (50 or 500 µg/kg) was administered in bolus by injecting the working solution (3.3 ml/kg) via the peritoneal catheter. Control mice received vehicle. The amount of ethanol administered by this and all other administration regimens caused neither detectable hemolysis nor any sign of intoxication.

Intravenous AMG0347 to rats. Working solutions containing AMG0347 at 30–1500 µg/ml and ethanol at 50% were prepared. The solutions were infused via the venous catheter at a rate of 167 $\mu l \cdot kg^{-1} \cdot min^{-1}$ for 2 min; the dose of AMG0347 infused by this regimen ranged from 10 to 500 µg/kg. To administer a lower dose (6 µg/kg), a working solution of AMG0347 (18 µg/ml) in 20% ethanol was infused at the same rate. Control rats were infused with the corresponding vehicle (50 or 20% ethanol in saline).

Intracerebroventricular AMG0347 to rats. A working solution containing AMG0347 at 1 µg/µl and ethanol at 50% was prepared. By infusing this solution into the lateral ventricle (1 µl/min for 2 min), a total dose of 6 µg/kg AMG0347 was delivered intracerebroventricularly. Control rats were infused with the vehicle (50% ethanol in saline). The infusions were performed via an injector needle (Plastics One) fitted into the preimplanted guide cannula. The injector protruded 2 mm beyond the end of the guide cannula (thus reaching the lateral ventricle); the injector was fitted to the guide at least 2 h before the infusion.

Intrathecal AMG0347 to rats. A working solution of AMG0347 (40 µg/ml) in 25% ethanol was prepared. By infusing this solution (25 µl/min) for 2 min via the thecal catheter, 6 µg/kg AMG0347 were delivered intrathecally. Control rats were infused with the vehicle (25% ethanol).

Intraperitoneal RTX to mice. RTX from *Euphorbia poisonii* was purchased from Sigma-Aldrich (St. Louis, MO). An ethanolic stock solution of RTX (20 µg/ml) was prepared, aliquoted, and stored at −80°C. The stock was diluted with ethanol and saline to give a working solution of RTX (150 ng/ml) in 25% ethanol. This solution was injected (3.3 ml/kg) via the peritoneal catheter. The RTX dose (500 ng/kg) delivered was below the minimal dose known to cause long-term desensitization (Dogan et al., 2004) but was within the dose range known to cause short-term hypothermia in mice (Shimizu et al., 2005). Control mice were injected with the vehicle (25% ethanol).

"Fake" intraperitoneal administration to mice (needle prick). A mouse was pricked with a sterile 26 gauge needle in the abdomen (no drug injected) to cause stress-associated hyperthermia.

Desensitization of TRPV1 channels
To cause localized (intra-abdominal) or systemic desensitization of TRPV1 channels, rats were injected with RTX intraperitoneally at a dose of 20 or 200 µg/kg, respectively (Dogan et al., 2004). A working solution of RTX (20 or 180 µg/ml) containing 20% ethanol was prepared. Because desensitizing doses of RTX cause excessive pain and discomfort, the working solution (or the vehicle) was injected (1 ml/kg; needle prick) in rats under ketamine–xylazine–acepromazine (55.6, 5.5, and 1.1 mg/kg, respectively, i.p.) anesthesia. The 20 µg/kg dose was delivered by a single injection of the 20 µg/ml solution, whereas the 200 µg/kg dose was delivered by injecting the 180 µg/ml solution 24 h after injection of the 20 µg/ml solution.

Desensitization tests
A battery of five tests was developed and used to confirm TRPV1 desensitization in different bodily compartments.

Eye-wiping test. After topical application of an irritant (e.g., a vanilloid compound) to the eye, a rat instinctively wipes the stimulated eye with the ipsilateral front paw, a response known to involve the TRPV1 channel (Dogan et al., 2004; Gavva et al., 2005b). To test whether TRPV1 channels in the cornea are desensitized, a drop (20 µl) of a solution of RTX (2 µg/ml) in 10% ethanol was applied to the cornea, and eye-wiping movements were counted for 5 min.

Centrally induced vasodilation test. Minute, systemically ineffective amounts of intrabrain capsaicin cause tail-skin vasodilation (Hori, 1984). To test whether TRPV1 channels in the brain are desensitized, a rat was placed in the thermocouple-respirometry setup at a slightly subneutral T_a (22°C) and infused intracerebroventricularly with capsaicin (25 µg) in 50% ethanol, while the T_{sk}, T_b, and T_a were monitored.

Bezold–Jarisch reflex test. The Bezold–Jarisch reflex consists of a triad of responses (apnea, bradycardia, and hypotension) triggered when sensory nerve endings located in the right atrium and pulmonary capillaries are stimulated by selected chemical irritants, capsaicin included (Aviado and Guevara-Aviado, 2001). Selective desensitization of cardiopulmonary af-

ferents blocks this reflex (Gu et al., 2005). To test whether TRPV1 channels in the right heart and pulmonary vessels were desensitized, a rat was placed in the thermocouple-respirometry setup at a neutral T_a (24°C) and injected with capsaicin (10 μg/kg) in 1% ethanol intravenously (i.e., in the superior vena cava), whereas the pulsatile arterial blood pressure was monitored using the Datamax blood-pressure-monitoring system (Columbus Instruments, Columbus, OH).

Hot-plate test. TRPV1 channels in the skin are involved in the so-called hot-plate response to noxious heat (Almasi et al., 2003). To test whether TRPV1 channels in the skin are desensitized, a rat was transferred from its home cage to a hot-plate apparatus (IITC Life Sciences, Woodland Hills, CA), the floor of which was maintained at 55°C. The time taken by the rat to respond with either hindpaw licking, hindpaw flicking, or jumping (the response latency) was measured. To prevent injury, rats that did not respond within 30 s (the cutoff time) were removed from the hot plate, and their response latency was considered 30 s.

Writhing test. Rodents injected intraperitoneally with irritants display episodes of abdominal muscle contraction (writhing response), a response that is drastically inhibited by TRPV1 blockade or desensitization (Ikeda et al., 2001). To test whether TRPV1 channels in the abdominal cavity are desensitized, a rat was injected intraperitoneally with RTX (0.1 μg/kg) in 10% ethanol, and the number of writhing episodes (abdominal muscle contraction associated with hindlimb extension) was counted for 10 min.

AMG0347 determination

The rats were anesthetized with ketamine–xylazine–acepromazine (5.56, 0.55, and 0.11 mg/kg, i.v., respectively), and arterial blood (3 ml) was collected by cardiac puncture and transferred to Microtainer tubes containing lithium heparin (BD, Franklin Lakes, NJ). The tubes were centrifuged (5000 × g, 10 min, 4°C), and the plasma was transferred to cryogenic vials and stored at −80°C. Immediately after blood was withdrawn from a rat, the animal was perfused through the left ventricle (right atrium cut) with 100 ml of saline. The brain was removed, weighed, frozen in liquid nitrogen, and stored at −80°C. The amount of AMG0347 present in a sample of plasma or brain tissue was assayed by HPLC-MS according to standard Amgen procedures.

Data processing and analysis

The heat loss index (HLI) was calculated according to the following formula: HLI = $(T_{sk} − T_a)/(T_b − T_a)$ (Romanovsky et al., 2002). Oxygen consumption (VO_2) was calculated by comparing the oxygen fraction (FO_2) in the air exiting a chamber containing a rat (FO_{2-rat}) to that exiting an empty chamber ($FO_{2-chamber}$). The following formula was used: $VO_2 = [$air flow × $(FO_{2-chamber} − FO_{2-rat})]/\{1 − [(1 − $respiratory quotient$) × FO_{2-chamber}]\}/$rat mass, where the respiratory quotient was considered to be 0.71. The equation term that includes the respiratory quotient accounts for the fact that CO_2 produced by the rat was not extracted from the air passing though the oxygen analyzer in our experimental setup. Mean arterial pressure was calculated from the time integral of the instantaneous pressure. The pain index was calculated according to the following formula: pain index = (cutoff time − response latency)/cutoff time. The responses were compared by one-way or two-way ANOVA, as appropriate, using Statistica AX'99 (StatSoft, Tulsa, OK). Results are reported as means ± SE.

Results

AMG0347 is a potent and selective TRPV1 antagonist *in vitro*

The ability of AMG0347 to block TRPV1 channel activation by heat (45°C), protons (pH 5), or capsaicin (500 nM) was studied in cultured Chinese hamster ovary cells stably transfected with the rat or human TRPV1 channel using the $^{45}Ca^{2+}$ uptake assay. AMG0347 inhibited activation of the rat TRPV1 channel by heat (IC_{50} = 0.2 nM), protons (IC_{50} = 0.8 nM), or capsaicin (IC_{50} = 0.7 nM) in a concentration-dependent manner (Fig. 1*B*). AMG0347 also inhibited all three modes of activation of the human TRPV1 channel with similar potencies (data not shown). The potency of AMG0347 was greater than that of other known
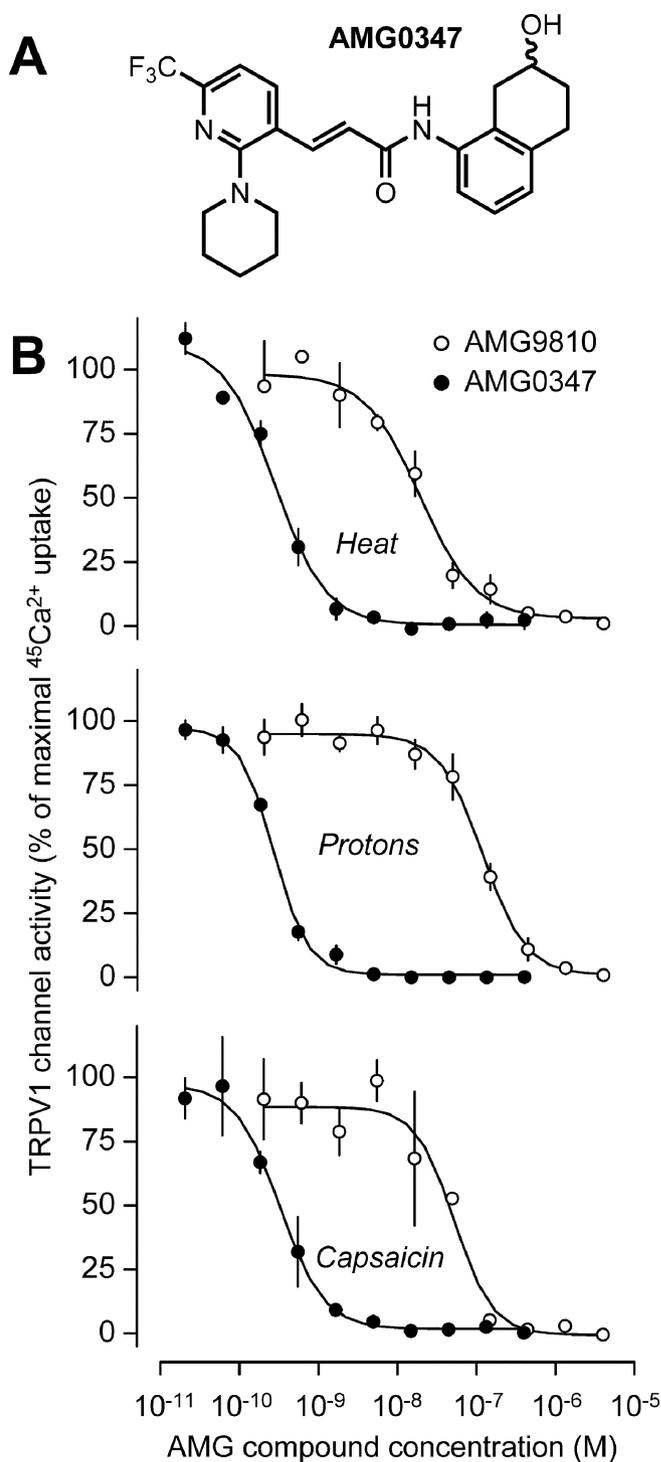
Figure 1. Chemical structure and *in vitro* pharmacology of AMG0347. ***A***, Structural formula of AMG0347 as confirmed by spectral analysis (supplemental Materials and Methods, available at www.jneurosci.org as supplemental material). ***B***, Concentration-dependent effects of AMG0347 on the activation of the TRPV1 channel by heat, protons, and capsaicin. For comparison, the effects of AMG9810 on channel activation by the same stimuli are shown. Channel activation was assessed based on the uptake of $^{45}Ca^{2+}$ by cultured Chinese hamster ovary cells stably transfected with the rat TRPV1 channel. The $^{45}Ca^{2+}$ uptake assay was conducted three times for each AMG compound–stimulus combination.

TRPV1 antagonists, including AMG9810 (Gavva et al., 2005b). Schild analysis (which evaluates the effect of the concentration of an agonist on a concentration-dependent effect of an antagonist) revealed that AMG0347 is a competitive antagonist (slope,
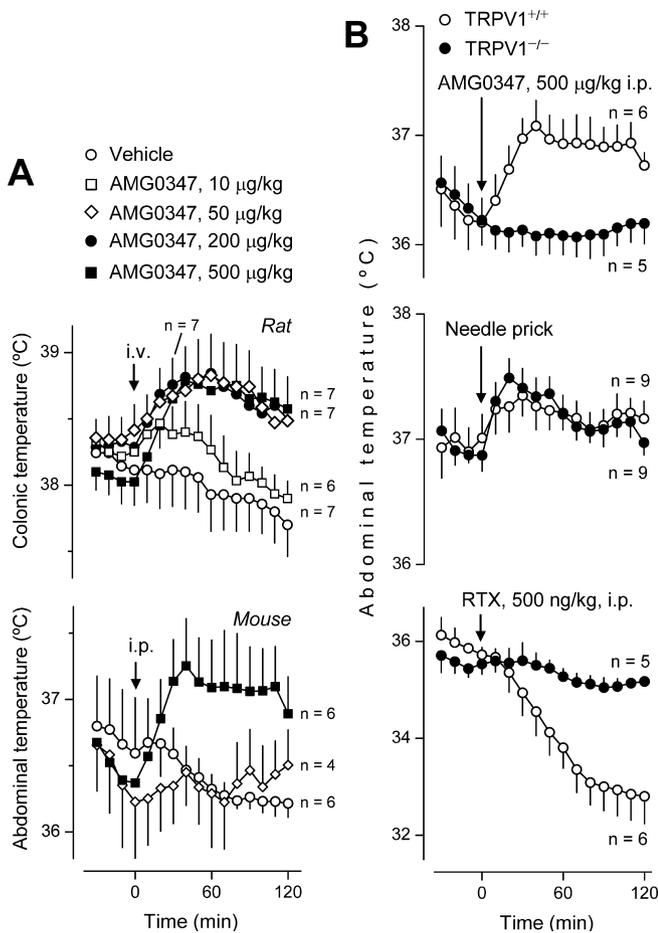
Figure 2. AMG0347 produces hyperthermia in wild-type rats and mice but not in TRPV1-deficient mice. ***A***, Effects of intravenous AMG0347 (doses indicated) or its vehicle on the colonic (deep body) temperature of rats at a neutral T_a of 28°C and on the abdominal (deep body) temperature of mice at a neutral T_a of 31°C. ***B***, Effects of AMG0347, abdominal needle prick, or RTX on the abdominal temperature of $TRPV1^{+/+}$ (wild-type) and $TRPV1^{-/-}$ (TRPV1-deficient) mice. When the stimulus was expected to result in hyperthermia (AMG0347 administration and needle prick), the experiment was conducted at a neutral T_a (31°C); when the stimulus was expected to result in hypothermia (RTX), the experiment was performed at a subneutral T_a (26°C). The number of animals in each group (n) is indicated.

−1.01; pK_b = 9.38) of capsaicin activation of the TRPV1 channel. Importantly, AMG0347 did not block other TRP channels, including TRPV2, TRPV3, TRPV4, TRP ankyrin-1, and TRP melastatin-8 (IC_{50} > 10 μM).

AMG0347 produces hyperthermia in rats and mice

Next, we studied the effect of AMG0347 on T_b *in vivo*. To avoid the development of stress hyperthermia, AMG0347 (or its vehicle) was infused in Wistar rats via a preimplanted venous catheter. Because the same animal has different thermoneutral zones (TNZs) in different experimental setups (Romanovsky et al., 2002; Rudaya et al., 2005) and because several setups were used in the present study, we always specify at which T_a the experiment was performed and how this T_a relates to the TNZ. The effect of AMG0347 on T_b of rats was studied in what we call the thermocouple-respirometry setup at T_a of 28°C, which is the upper limit of the TNZ of rats in this setup (for details, see Materials and Methods). Under these conditions, the vehicle-treated rats presented a slight decrease in colonic temperature (an index of T_b) over the course of the experiment (Fig. 2A). Such a decrease often occurs in rats and mice during the light phase of the day,

presumably reflecting the circadian rhythm of T_b (Steiner et al., 2004). In AMG0347-treated rats, T_b started to increase at ~10 min after the onset of the infusion, reached a peak between 20 and 60 min, and then gradually returned to the baseline level. Both the magnitude and timing of the T_b peak were dose dependent. At 10 μg/kg intracerebroventricularly, AMG0347 caused a small (~0.3°C; p = 2.7 × 10^{-2}) T_b rise that peaked at ~20 min. At 50 μg/kg intravenously, the T_b rise was greater (~0.6°C; p = 2.0 × 10^{-5}) and peaked at ~60 min. The T_b responses to even higher doses (200 and 500 μg/kg, i.v.) did not differ from the response to 50 μg/kg. That AMG0347 increased T_b at a dose as low as 10 μg/kg makes the potency of this drug to cause hyperthermia at least 300 times greater than the potency of any other TRPV1 antagonist tested thus far (Swanson et al., 2005; Gavva et al., 2007). AMG0347 was also found to be more potent than other TRPV1 antagonists to suppress thermal hyperalgesia in rats (Gavva et al., 2005a).

We then studied the effects of AMG0347 on T_b in mice. These experiments were conducted in the telemetry setup at T_a of 31°C, which is neutral in this setup (see Materials and Methods). Like the rats, the mice were infused with AMG0347 (or its vehicle) in a nonstressful manner, via a preimplanted catheter. However, to avoid technical problems and complications associated with the catheterization of the small and fragile veins of a mouse, the catheter was implanted in the peritoneal cavity. Neither vehicle nor AMG0347 at 50 μg/kg increased the abdominal temperature (also an index of T_b) of the mice (Fig. 2A). Only at 500 μg/kg did AMG0347 cause a significant (p = 5.4 × 10^{-3}) T_b rise. Differences in the route of administration are likely to explain why the dose of AMG0347 needed to cause hyperthermia was somewhat higher in the mouse experiments (intraperitoneal infusion) than in the rat experiments (intravenous infusion).

AMG0347 does not cause hyperthermia in the absence of the TRPV1 channel

In previous papers (Swanson et al., 2005; Gavva et al., 2007), no data were reported to show whether TRPV1 antagonists cause hyperthermia by acting on the TRPV1 channel or whether the hyperthermic effect of these drugs is TRPV1 unrelated. If AMG0347 causes hyperthermia by acting on the TRPV1 channel, such a hyperthermic response should not occur in TRPV1-deficient animals. Here, we showed that mice that carry a homozygous targeted null mutation in the TRPV1 gene ($TRPV1^{-/-}$ mice) did not respond to AMG0347 with hyperthermia, whereas their nonmutant ($TRPV1^{+/+}$) littermates did (p = 5.4 × 10^{-3}) (Fig. 2B). The $TRPV1^{-/-}$ mice, however, were as capable as the $TRPV1^{+/+}$ mice to increase their T_b (p = 2.2 × 10^{-5} for both) in response to a distinct stimulus, needle prick. That $TRPV1^{-/-}$ mice did not respond to the TRPV1 agonist RTX (500 ng/kg, i.p.) with pronounced hypothermia confirms the absence of the TRPV1 channel in the animals used.

AMG0347-induced hyperthermia: thermoeffector pattern

The thermocouple-respirometry setup was used to monitor T_b, T_{sk}, and VO_2 in loosely restrained rats kept at a constant T_a; under these conditions, T_b regulation depends exclusively on autonomic effectors. The HLI [$(T_{sk} - T_a)/(T_b - T_a)$] was used as an index of tail-skin vasomotion (Romanovsky et al., 2002); VO_2 was used as an index of thermogenesis. Theoretically, VO_2 can reflect changes in both shivering and nonshivering thermogenesis. In small rodents, however, nonshivering thermogenesis is of greater importance (Cannon and Nedergaard, 2004). Because the activity of autonomic effectors depends on the thermal environ-

ment (Romanovsky et al., 2002), the experiments were conducted at several T_a values: 28°C (the upper end of the TNZ in this setup), 24°C (the lower end of the TNZ), or 17°C (6°C below the TNZ). The results of this experiment are shown in Figure 3*A*. Before receiving AMG0347 or its vehicle, the rats exhibited pronounced tail-skin vasodilation (a high HLI) at 28°C, modest vasodilation (an intermediate HLI) at 24°C, and maximal vasoconstriction (the lowest HLI) at 17°C. Thermogenesis (VO_2) was lower within the TNZ (28°C and 24°C) than at the subneutral T_a of 17°C. At no T_a did the vehicle cause a hyperthermic response, whereas AMG0347 caused significant T_b rises at all T_a values tested ($p = 2.0 \times 10^{-5}$ at 28°C; $p = 9.0 \times 10^{-6}$ at 24°C and 17°C). Although T_a affected neither the magnitude nor the time course of the hyperthermic response to AMG0347, it modified the thermoeffector profile of the response. At 28°C, AMG0347 elicited skin vasoconstriction [significant ($p = 3.4 \times 10^{-4}$) fall in the HLI] and tended to elevate thermogenesis (VO_2). At 24°C, AMG0347 evoked skin vasoconstriction ($p = 1.8 \times 10^{-2}$) and increased thermogenesis significantly ($p = 5.9 \times 10^{-3}$). At 17°C, AMG0347 strongly activated thermogenesis ($p = 5.4 \times 10^{-4}$) but did not cause any additional tail-skin vasoconstriction.

The effect of AMG0347 on a behavioral response (selection of a preferred T_a) was studied in a multichannel thermogradient setup. After the intravenous administration of the vehicle, the rats showed a transient stress hyperthermia and a slight decrease in the preferred T_a (supplemental Fig. 1, available at www.jneurosci.org as supplemental material), which was attributable to the fact that injection in this setup involved handling. Rats treated with a high dose (500 μg/kg, i.v.) of AMG0347 exhibited a larger and longer rise in T_b ($p = 9.0 \times 10^{-6}$), but even such a high dose of AMG0347 did not cause any effect of its own on the preferred T_a.

AMG0347 hyperthermia is independent of basal T_b or T_{sk}

If the TRPV1 channel is indeed activated *in vivo* by relatively low temperatures [perhaps as low as 34°C (Ni et al., 2006)], it is tempting to hypothesize that the thermoregulatory response to TRPV1 antagonists is related to a suppression of the activation of this channel by physiological temperatures. Because a higher temperature is expected to cause a stronger thermal activation of the TRPV1 channel, blocking thermal activation should cause a stronger response at a higher T_b (if the responsible TRPV1 channels are located in the body core and are activated by T_b) or at a higher T_{sk} (if the responsible TRPV1 channels are located in the body surface and are activated by T_{sk}). Hence, if AMG0347-induced hyperthermia occurs as a result of the blockade of thermal activation of the TRPV1 channel, there must be a positive correlation between the magnitude of AMG0347 hyperthermia and the initial (at the time of drug administration) values of T_b and/or T_{sk}. By subjecting the data presented in Figure 3*A* to linear correlation analyses, we found a tendency ($p = 7.8 \times 10^{-2}$) for a negative correlation between the maximal value of change in T_b (between 10 and 180 min after AMG0347 administration) and
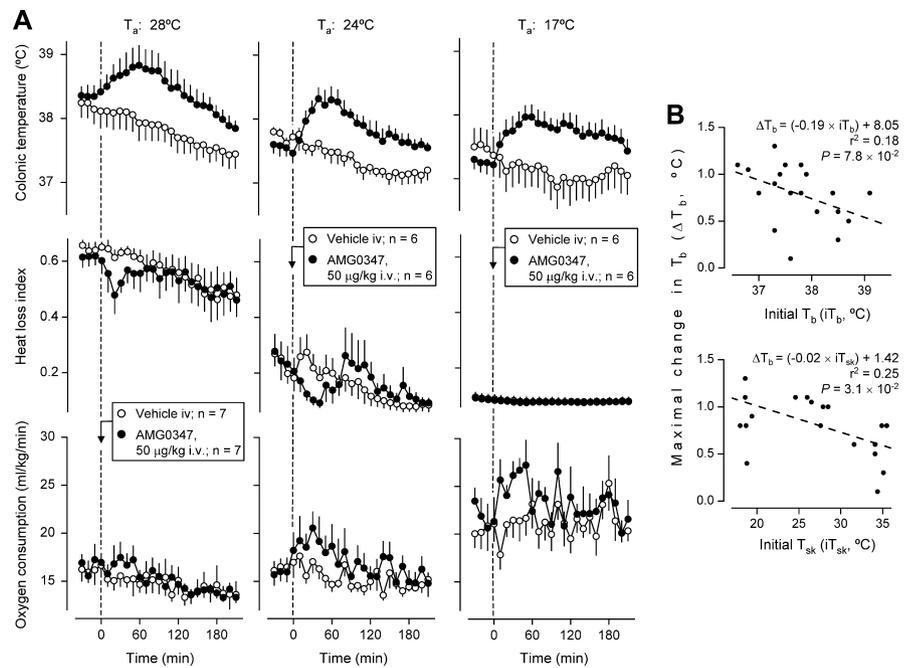
Figure 3. AMG0347 hyperthermia is brought about by activation of autonomic thermoeffectors and is independent of basal T_b and T_{sk}. *A*, Effects of AMG0347 or its vehicle on the colonic temperature, heat loss index, and oxygen consumption of rats at T_a of 28°C (upper end of the TNZ), 24°C (lower end of the TNZ), or 17°C (below the lower end of the TNZ). Colonic temperature is an index of deep T_b, the heat loss index is an index of skin vasodilation, and oxygen consumption is an index of thermogenesis. *B*, Results of a linear correlation analysis between the magnitude of AMG0347-induced hyperthermia and the values of either T_b or T_{sk} immediately before AMG0347 administration. Based on the data presented in *A*.

the initial value of T_b, and a weak negative correlation ($p = 3.1 \times 10^{-2}$) between the maximal change in T_b and initial T_{sk} (Fig. 3*B*). These results reject the original hypothesis. Hence, TRPV1 channels are tonically activated by nonthermal stimuli, and the blockade of this nonthermal activation causes a rise in T_b.

AMG0347 causes hyperthermia by acting outside the CNS

We then attempted to determine the location of TRPV1 channels responsible for the hyperthermic effect of AMG0347. First, we determined whether AMG0347 crosses the blood–brain barrier. Rats were injected with AMG0347 (50 μg/kg, i.v.), and their arterial blood and brains were harvested 60 min later, i.e., at the time corresponding to the peak of AMG0347-induced hyperthermia. At that time point, the concentration of the drug in the brain (4.1 ± 0.6 μg/g; $n = 4$) was only 3.4 times lower than the concentration in the blood plasma (14.0 ± 1.6 μg/ml; $n = 4$). Because AMG0347 crosses the blood–brain barrier, it is unclear whether it causes hyperthermia by acting inside or outside the CNS. We then investigated whether AMG0347 can cause hyperthermia by acting inside the brain or spinal cord. If one of these sites were a primary site of the hyperthermic action of AMG0347, the intracerebroventricular or intrathecal administration of AMG0347 would cause hyperthermia at doses substantially lower (perhaps one to two orders of magnitude) than the minimally effective intravenous dose of 10 μg/kg (Fig. 2*A*). The experiment was conducted in the thermocouple-respirometry setup at T_a of 24°C. At a dose as high as 6 μg/kg, AMG0347 administered intracerebroventricularly, intrathecally, or intravenously did not produce any significant change in T_b, although a tendency for an increase in T_b was observed after either the intracerebroventricular or intravenous administration (supplemental Fig. 2, available at www.jneurosci.org as supplemental material). Because intravenous AMG0347 showed a tendency to increase T_b at the 6

Pretreatment
○ Vehicle i.p.; n = 8
● RTX, 20 µg/kg i.p.; n = 7

▼ AMG0347, 50 µg/kg i.v.
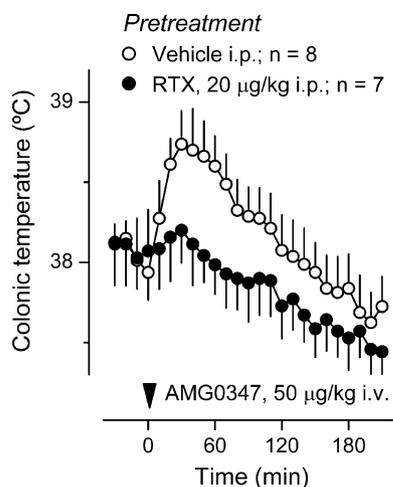
Figure 4. AMG0347 hyperthermia is absent in rats with localized intra-abdominal TRPV1 desensitization. The colonic temperature response of rats pretreated with RTX (20 µg/kg, i.p.) or its vehicle to administration of AMG0347 at thermoneutrality (T_a of 24°C) is shown.

µg/kg dose (and a significant effect at 10 µg/kg), there was no reason to further increase the dose of AMG0347 in this experiment. Clearly, AMG0347 is not more effective in causing hyperthermia when administered into the brain or spinal cord than when administered systemically.

AMG0347 causes hyperthermia by acting on intra-abdominal targets

Outside the CNS, the TRPV1 channel is abundant in primary sensory neurons. Many TRPV1-containing afferents travel within the spinal nerves and the vagus and innervate the abdominal viscera (Zhang et al., 2004; Hwang et al., 2005; Bielefeldt et al., 2006). To test the hypothesis that AMG0347 causes hyperthermia by acting on intra-abdominal targets, we induced localized desensitization of TRPV1 channels in the abdominal viscera, as in the past (Dogan et al., 2004). This method is based on the well established fact that a single dose of a TRPV1 agonist (e.g., capsaicin and RTX) can make the TRPV1 channel unresponsive to subsequent stimulation. To cause localized, intra-abdominal desensitization of TRPV1 channels, a low desensitizing dose (20 µg/kg, i.p.) of RTX was injected 10 d before studying the thermal response to AMG0347 (50 µg/kg, i.v.) in the thermocouple-respirometry setup at T_a of 24°C. Whereas vehicle-pretreated rats responded to AMG0347 with a typical hyperthermic response, localized desensitization of abdominal viscera with RTX completely abolished this hyperthermia ($p = 9.0 \times 10^{-6}$) (Fig. 4).

We then confirmed that TRPV1 desensitization in the model used was indeed restricted to the abdominal cavity. For this, we performed a battery of tests (Fig. 5) in this model of localized desensitization, as well as in rats with systemic desensitization of TRPV1 channels [caused by a high (200 µg/kg, i.p.) dose of RTX (Dogan et al., 2004)] and in nondesensitized rats (treated with the vehicle). All tests were conducted 6–13 d after the initial administration of RTX or its vehicle. The following tests were used (as explained in Materials and Methods): the eye-wiping test (determines the sensitivity of TRPV1 channels in the eye); the centrally induced tail-vasodilation test (determines the sensitivity of TRPV1 channels in the brain); the Bezold–Jarisch reflex test (determines the sensitivity of TRPV1 channels in the heart and lungs); the hot-plate test (assesses the sensitivity of TRPV1 channels in the skin, primarily of the paws); and the writhing test

(determines the sensitivity of TRPV1 channels in the peritoneal cavity). In the rats with systemic desensitization, the responsivity of TRPV1 channels was drastically reduced (compared with the vehicle-treated rats) in all compartments studied [namely, the eye ($p = 1.5 \times 10^{-2}$), the brain ($p = 2.2 \times 10^{-5}$), the heart and lungs ($p = 3.6 \times 10^{-3}$), the skin ($p = 1.3 \times 10^{-4}$), and the peritoneum ($p = 1.3 \times 10^{-3}$)], thus confirming a sufficient sensitivity of all of the tests. In rats with localized desensitization of intra-abdominal TRPV1 channels, the writhing test confirmed a drastic reduction in the responsivity of these channels in the abdominal compartment ($p = 1.4 \times 10^{-4}$), but no other compartment was affected.

Discussion

It is well known that experimental animals, including rats and mice, respond to vanilloid agonists such as capsaicin and RTX with a fall in T_b (Dogan et al., 2004; Almeida et al., 2006b). The hypothermic action of these compounds is known to result from pharmacological activation of the TRPV1 channel (Caterina et al., 2000; Dogan et al., 2004; Shimizu et al., 2005). Surprisingly, whether the TRPV1 channel has a physiological role in T_b regulation is unknown. To address this question, we used a newly synthesized, highly potent TRPV1 antagonist, AMG0347. We found that AMG0347 causes hyperthermia in rats and mice at doses as low as 10 µg/kg intravenously. Although the previous studies with capsazepine [a "traditional" TRPV1 antagonist, which is particularly ineffective in rodents (McIntyre et al., 2001)] did not find such an effect (Dogan et al., 2004; Shimizu et al., 2005), two recent studies that used several chemotypes of novel TRPV1 antagonists did (Swanson et al., 2005; Gavva et al., 2007). However, both recent studies used much higher doses (3–30 mg/kg) of TRPV1 antagonists and did not use knock-out animals to show that the effect revealed was indeed mediated by the TRPV1 channel. Here, we show unequivocally that TRPV1 antagonist-induced hyperthermia is indeed mediated by the TRPV1. We found that TRPV1-deficient mice do not respond to AMG0347 with hyperthermia, although they are capable of increasing their T_b in response to a TRPV1-independent stimulus (needle prick). Interestingly, there are also two studies (Jancso-Gabor et al., 1970; Woods et al., 1994) that found transient hyperthermia in rats during the first 2–3 d after the administration of desensitizing doses of capsaicin or RTX, a finding that agrees with the recently discovered hyperthermic effect of novel TRPV1 antagonists. We conclude that TRPV1 channels are tonically activated *in vivo*, thus constantly suppressing T_b and keeping it at its normal level; when TRPV1 channels are blocked, this suppression is removed, and T_b increases.

What are the mechanisms underlying the revealed thermoregulatory involvement of the TRPV1 channel? The popular set point-based model of T_b regulation, which postulates that an integrated signal is generated by a single controller and drives the activity of all thermoeffectors, is now giving way to a new model (Romanovsky, 2007). According to the new model, thermoeffectors are driven by parallel, relatively independent neuronal (afferent–efferent) loops that talk to each other primarily via a common controlled variable, T_b. Hence, it is important to identify the thermoeffector loop(s) affected by TRPV1 antagonists. We found that the hyperthermic effect of AMG0347 in rats occurs as a result of tail-skin vasoconstriction and activation of thermogenesis, two major autonomic cold-defense effectors (Romanovsky, 2006). Similar to the hyperthermic responses to prostaglandin E_2 and cholecystokinin octapeptide (Crawshaw and Stitt, 1975; Szelenyi et al., 1992), the contributions of skin vasoconstriction and thermogenesis to the

overall rise in T_b differed at different T_a values. Although AMG0347 altered the activity of autonomic thermoeffectors, it did not affect an important behavioral thermoeffector (thermal preference), even at a high dose. These findings suggest that AMG0347 triggers the hyperthermic response by blocking activation of the TRPV1 channels located on structures preferentially involved in the autonomic (but not behavioral) thermoeffector loops.

A recent study (Gavva et al., 2007) hypothesized that TRPV1 antagonists increase T_b by acting on the brain circumventricular organs, including the organum vasculosum of the lamina terminalis (OVLT) that forms the anterior wall of the third brain ventricle. This hypothesis agrees with the fact that the anterior preoptic hypothalamus (that contains the OVLT) is more important for the control of autonomic thermoeffectors than for the control of thermotaxis (Almeida et al., 2006a) and with the fact that electrolytic lesions of the OVLT and neighboring structures readily cause hyperthermia (Romanovsky et al., 2003). We found, however, that AMG0347 fails to cause marked hyperthermia when infused via the route (intracerebroventricular) that provides good access to the OVLT and other circumventricular structures. We also found that administration of AMG0347 into the spinal cord (intrathecally) is no more effective in causing hyperthermia than the intravenous administration of this drug. These findings suggest that AMG0347 causes hyperthermia by blocking TRPV1 channels outside the CNS.

Based on our experiments with localized intra-abdominal desensitization of TRPV1 channels by RTX, we propose that the site of the hyperthermic action of AMG0347 lies within the abdominal cavity. The abdominal viscera are densely innervated by TRPV1-positive afferents. For example, the TRPV1 channel is present in at least 60% of the spinal nerve afferents serving the upper gastrointestinal tract, large intestine, and urinary bladder, whereas it is present in 30% or less of the spinal afferents serving the skin or skeletal muscles (Schicho et al., 2004; Hwang et al., 2005; Christianson et al., 2006). In addition to the spinal nerves, the vagus nerve serves the abdominal viscera, and at least 20% of the vagal afferents innervating the upper gastrointestinal tract contain the TRPV1 channel (Schicho et al., 2004; Zhang et al., 2004; Bielefeldt et al., 2006). The hypothesis that AMG0347 causes hyperthermia by blocking TRPV1 channels on afferent fibers innervating the abdominal viscera also agrees with our data showing that the hyperthermic response to this drug involves activation of autonomic thermoeffectors but does not involve thermoregulatory locomotion. Indeed, the latter behavioral response is triggered
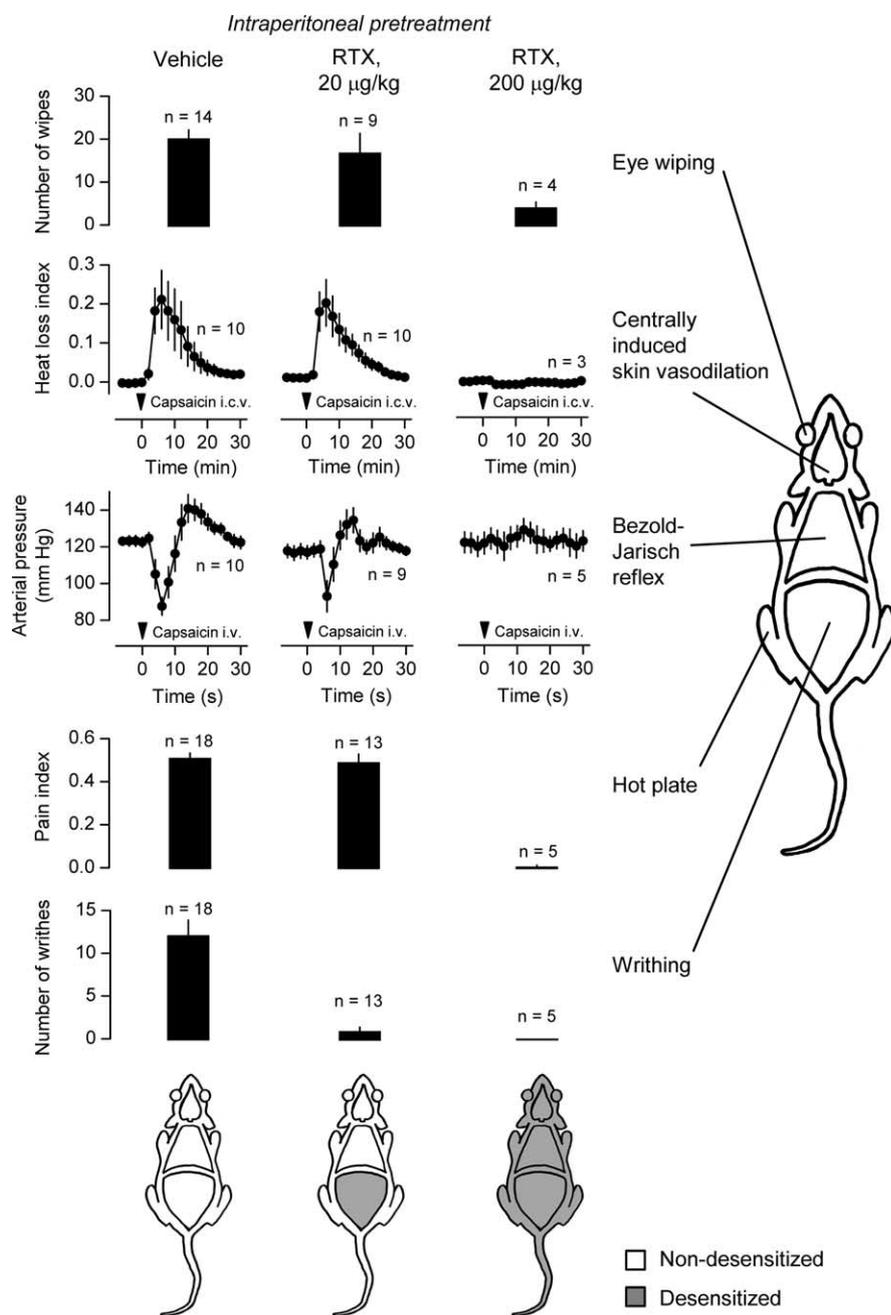
Figure 5. Sites of TRPV1 desensitization in RTX-pretreated rats. The sensitivity of TRPV1 channels in different bodily compartments was determined in vehicle-pretreated rats, in rats pretreated with a low desensitizing dose (20 μg/kg, i.p.) of RTX, and in rats pretreated with a high dose (200 μg/kg, i.p.) of RTX. Five tests were performed: the eye-wiping test (determines the sensitivity of TRPV1 channels in the eye); the centrally induced tail-vasodilation test (determines the sensitivity of TRPV1 channels in the brain); the Bezold–Jarisch reflex test (determines the sensitivity of TRPV1 channels in the heart and lungs); the hot-plate test (assesses the sensitivity of TRPV1 channels in the skin, primarily of the paws); and the writhing test (determines the sensitivity of TRPV1 channels in the peritoneal cavity). For methodological details, see Materials and Methods. The results of all tests are summarized in the schematics at the bottom.

almost exclusively by changes in T_{sk} (detected by skin nerves), whereas core temperatures (detected by visceral and deep somatic nerves) seem relatively more important for triggering autonomic thermoeffectors (for a recent review, see Romanovsky, 2007). It should also be considered that the TRPV1 channel is expressed by some non-neuronal cells, e.g., the gastric and urinary bladder epitheliocytes (Birder et al., 2001; Faussone-Pellegrini et al., 2005), but the level of TRPV1 channel expression in afferent neurons is at least 30 times higher than that in any other cell population (Sanchez et al., 2001).

Perhaps the most unexpected finding of the present study is the lack of a positive correlation between the magnitude of AMG0347-induced hyperthermia and the rats' T_b or T_{sk}. This finding strongly suggests that the normally present tonic suppression of T_b occurs as a result of tonic activation of TRPV1 channels by nonthermal factors. Such factors may include protons (Caterina et al., 1997; Tominaga et al., 1998), inorganic cations (Ahern et al., 2005), and various lipid ligands such as anandamide (Zygmunt et al., 1999) and N-oleoyl-dopamine (Chu et al., 2003). Not only can these factors directly activate the TRPV1 channel, but they can also potentiate each other's actions in a synergistic manner (Tominaga et al., 1998). That many nonthermal signals originating in the abdominal viscera can affect thermoregulation is known. For instance, the intraduodenal infusion of hypertonic saline (Osaka et al., 2002), the intraportal infusion of glucose (Sakaguchi and Yamazaki, 1988), and distension of the stomach (Petervari et al., 2005) can all activate thermogenesis via the appropriate reflexes, whereas colorectal distension can trigger neuroreflexive skin vasoconstriction (Laird et al., 2006).

Whereas recent studies have shown an involvement of ThermoTRP channels [namely, TRPV3 (Moqrich et al., 2005) and TRPV4 (Lee et al., 2005)] in thermotaxis, this study shows that the activity of a ThermoTRP channel modulates the level at which T_b is maintained. It shows that TRPV1 channels located in the abdominal viscera and activated by presently unknown nonthermal factors tonically suppress T_b by inhibiting the two major cold-defense autonomic effectors: thermoregulatory skin vasoconstriction and thermogenesis. When TRPV1 channels are blocked (e.g., by AMG0347), these two thermoeffectors are disinhibited, and T_b increases.

Perspectives

From the point of view of additional development of TRPV1 antagonists as analgesic and anti-inflammatory drugs, their hyperthermic action, the major focus of the present study, poses a highly undesired on-target side effect. One potential way to dissociate the analgesic and hyperthermic effects of TRPV1 antagonists is to take advantage of the fact that the hyperthermic effect fades away with repeated administration of an antagonist, whereas the analgesic effect shows no attenuation. Such a dissociation seen for two TRPV1 antagonists (N. R. Gavva, A. W. Bannon, D. N. Hovland Jr, S. G. Lehto, S. Surapaneni, D. C. Immke, C. Henley, A. Bak, J. Davis, G. Hever, L. Klionsky, R. Kuang, N. Ernst, R. Tamir, J. Wang, W. Wang, G. Zajic, D. Zhu, M. H. Norman, J.-C. Louis, E. Magal, and J. J. S. Treanor, unpublished observations) is consistent with observations in TRPV1-deficient mice: these animals present no thermoregulatory abnormalities (Szelenyi et al., 2004; Iida et al., 2005), but their responses to painful stimuli are suppressed (Caterina et al., 2000; Davis et al., 2000). The present study may serve as a first step for developing alternative strategies for dissociating the hyperthermic and analgesic effects of TRPV1 antagonists. These strategies can be based on the following two findings of the present study: (1) the TRPV1-bearing cells that trigger the hyperthermic response to TRPV1 antagonists have a specific location (the peritoneal cavity), and (2) these cells are tonically activated by a certain class of stimuli (nonthermal). Specific recipes of how to translate this new knowledge into hyperthermia-free TRPV1 antagonist therapy remain to be developed.

References

Ahern GP, Brooks IM, Miyares RL, Wang XB (2005) Extracellular cations sensitize and gate capsaicin receptor TRPV1 modulating pain signaling. J Neurosci 25:5109–5116.

Almasi R, Petho G, Bolcskei K, Szolcsanyi J (2003) Effect of resiniferatoxin on the noxious heat threshold temperature in the rat: a novel heat allodynia model sensitive to analgesics. Br J Pharmacol 139:49–58.

Almeida MC, Steiner AA, Branco LG, Romanovsky AA (2006a) Neural substrate of cold-seeking behavior in endotoxin shock. PLoS ONE 1:e1.

Almeida MC, Steiner AA, Branco LG, Romanovsky AA (2006b) Cold-seeking behavior as a thermoregulatory strategy in systemic inflammation. Eur J Neurosci 23:3359–3367.

Aviado DM, Guevara-Aviado D (2001) The Bezold-Jarisch reflex. A historical perspective of cardiopulmonary reflexes. Ann NY Acad Sci 940:48–58.

Bielefeldt K, Zhong F, Koerber HR, Davis BM (2006) Phenotypic characterization of gastric sensory neurons in mice. Am J Physiol Gastrointest Liver Physiol 291:G987–G997.

Birder LA, Kanai AJ, de Groat WC, Kiss S, Nealen ML, Burke NE, Dineley KE, Watkins S, Reynolds IJ, Caterina MJ (2001) Vanilloid receptor expression suggests a sensory role for urinary bladder epithelial cells. Proc Natl Acad Sci USA 98:13396–13401.

Cannon B, Nedergaard J (2004) Brown adipose tissue: function and physiological significance. Physiol Rev 84:277–359.

Caterina MJ, Schumacher MA, Tominaga M, Rosen TA, Levine JD, Julius D (1997) The capsaicin receptor: a heat-activated ion channel in the pain pathway. Nature 389:816–824.

Caterina MJ, Leffler A, Malmberg AB, Martin WJ, Trafton J, Petersen-Zeitz KR, Koltzenburg M, Basbaum AI, Julius D (2000) Impaired nociception and pain sensation in mice lacking the capsaicin receptor. Science 288:306–313.

Christianson JA, McIlwrath SL, Koerber HR, Davis BM (2006) Transient receptor potential vanilloid 1-immunopositive neurons in the mouse are more prevalent within colon afferents compared to skin and muscle afferents. Neuroscience 140:247–257.

Chu CJ, Huang SM, De Petrocellis L, Bisogno T, Ewing SA, Miller JD, Zipkin RE, Daddario N, Appendino G, Di Marzo V, Walker JM (2003) N-oleoyldopamine, a novel endogenous capsaicin-like lipid that produces hyperalgesia. J Biol Chem 278:13633–13639.

Crawshaw LI, Stitt JT (1975) Behavioural and autonomic induction of prostaglandin E_1 fever in squirrel monkeys. J Physiol (Lond) 244:197–206.

Davis JB, Gray J, Gunthorpe MJ, Hatcher JP, Davey PT, Overend P, Harries MH, Latcham J, Clapham C, Atkinson K, Hughes SA, Rance K, Grau E, Harper AJ, Pugh PL, Rogers DC, Bingham S, Randall A, Sheardown SA (2000) Vanilloid receptor-1 is essential for inflammatory thermal hyperalgesia. Nature 405:183–187.

Dhaka A, Viswanath V, Patapoutian A (2006) TRP ion channels and temperature sensation. Annu Rev Neurosci 29:135–161.

Dogan MD, Patel S, Rudaya AY, Steiner AA, Szekely M, Romanovsky AA (2004) Lipopolysaccharide fever is initiated via a capsaicin-sensitive mechanism independent of the subtype-1 vanilloid receptor. Br J Pharmacol 143:1023–1032.

Faussone-Pellegrini MS, Taddei A, Bizzoco E, Lazzeri M, Vannucchi MG, Bechi P (2005) Distribution of the vanilloid (capsaicin) receptor type 1 in the human stomach. Histochem Cell Biol 124:61–68.

Garcia-Martinez C, Humet M, Planells-Cases R, Gomis A, Caprini M, Viana F, De La Pena E, Sanchez-Baeza F, Carbonell T, De Felipe C, Perez-Paya E, Belmonte C, Messeguer A, Ferrer-Montiel A (2002) Attenuation of thermal nociception and hyperalgesia by VR1 blockers. Proc Natl Acad Sci USA 99:2374–2379.

Gavva NR, Klionsky L, Qu Y, Shi L, Tamir R, Edenson S, Zhang TJ, Viswanadhan VN, Toth A, Pearce LV, Vanderah TW, Porreca F, Blumberg PM, Lile J, Sun Y, Wild K, Louis JC, Treanor JJ (2004) Molecular determinants of vanilloid sensitivity in TRPV1. J Biol Chem 279:20283–20295.

Gavva NR, Bannon AW, Tamir R, Wang Q, Zhu D, Le A, Youngblood B, Kuang R, Deng H, Wang J, Surapaneni S, Magal E, Louis J, Norman MH, Treanor JJ (2005a) Identification and biological evaluation of AMG0347 [(E)-n-(7-hydroxy-5,6,7,8-tetrahydronaphthalen-1-yl)-3-(2-(piperidin-1-yl)-6-(trifluoromethyl)pyridin-3-yl)acrylamide], a potent vanilloid receptor 1 antagonist. Soc Neurosci Abstr 31:292.16.

Gavva NR, Tamir R, Qu Y, Klionsky L, Zhang TJ, Immke D, Wang J, Zhu D, Vanderah TW, Porreca F, Doherty EM, Norman MH, Wild KD, Bannon AW, Louis JC, Treanor JJ (2005b) AMG 9810 [(E)-3-(4-t-butylphenyl)-N-(2,3-dihydrobenzo[b][1,4] dioxin-6-yl)acrylamide], a novel vanilloid receptor 1 (TRPV1) antagonist with antihyperalgesic properties. J Pharmacol Exp Ther 313:474–484.

Gavva NR, Bannon AW, Surapaneni S, Hovland Jr DN, Lehto SG, Gore A, Juan T, Deng H, Han B, Klionsky L, Kuang R, Le A, Tamir R, Wang J, Youngblood B, Zhu D, Norman MH, Magal E, Treanor JJS, Louis JC (2007) The vanilloid receptor TRPV1 is tonically activated *in vivo* and involved in body temperature regulation. J Neurosci 27:3366–3374.

Gu Q, Lin RL, Hu HZ, Zhu MX, Lee LY (2005) 2-aminoethoxydiphenyl borate stimulates pulmonary C neurons via the activation of TRPV channels. Am J Physiol Lung Cell Mol Physiol 288:L932–L941.

Hori T (1984) Capsaicin and central control of thermoregulation. Pharmacol Ther 26:389–416.

Hwang SJ, Oh JM, Valtschanoff JG (2005) Expression of the vanilloid receptor TRPV1 in rat dorsal root ganglion neurons supports different roles of the receptor in visceral and cutaneous afferents. Brain Res 1047:261–266.

Iida T, Shimizu I, Nealen ML, Campbell A, Caterina M (2005) Attenuated fever response in mice lacking TRPV1. Neurosci Lett 378:28–33.

Ikeda Y, Ueno A, Naraba H, Oh-ishi S (2001) Involvement of vanilloid receptor VR1 and prostanoids in the acid-induced writhing responses of mice. Life Sci 69:2911–2919.

Jancso-Gabor A, Szolcsanyi J, Jancso N (1970) Irreversible impairment of thermoregulation induced by capsaicin and similar pungent substances in rats and guinea-pigs. J Physiol (Lond) 206:495–507.

Laird AS, Carrive P, Waite PM (2006) Cardiovascular and temperature changes in spinal cord injured rats at rest and during autonomic dysreflexia. J Physiol (Lond) 577:539–548.

Lee H, Iida T, Mizuno A, Suzuki M, Caterina MJ (2005) Altered thermal selection behavior in mice lacking transient receptor potential vanilloid 4. J Neurosci 25:1304–1310.

McIntyre P, McLatchie LM, Chambers A, Phillips E, Clarke M, Savidge J, Toms C, Peacock M, Shah K, Winter J, Weerasakera N, Webb M, Rang HP, Bevan S, James IF (2001) Pharmacological differences between the human and rat vanilloid receptor 1 (VR1). Br J Pharmacol 132:1084–1094.

Moqrich A, Hwang SW, Earley TJ, Petrus MJ, Murray AN, Spencer KS, Andahazy M, Story GM, Patapoutian A (2005) Impaired thermosensation in mice lacking TRPV3, a heat and camphor sensor in the skin. Science 307:1468–1472.

Ni D, Gu Q, Hu HZ, Gao N, Zhu MX, Lee LY (2006) Thermal sensitivity of isolated vagal pulmonary sensory neurons: role of transient receptor potential vanilloid receptors. Am J Physiol Regul Integr Comp Physiol 291:R541–R550.

Osaka T, Kobayashi A, Inoue S (2002) Vago-sympathoadrenal reflex in thermogenesis induced by osmotic stimulation of the intestines in the rat. J Physiol (Lond) 540:665–671.

Petervari E, Garami A, Pakai E, Szekely M (2005) Effects of perineural capsaicin treatment of the abdominal vagus on endotoxin fever and on a non-febrile thermoregulatory event. J Endotoxin Res 11:260–266.

Pogatzki EM, Zahn PK, Brennan TJ (2000) Lumbar catheterization of the subarachnoid space with a 32-gauge polyurethane catheter in the rat. Eur J Pain 4:111–113.

Romanovsky AA (2006) Temperature regulation. In: Lecture notes on human physiology, Chap 23 (Petersen O, ed), pp 603–615. Oxford: Blackwell.

Romanovsky AA (2007) Thermoregulation: some concepts have changed. Functional architecture of the thermoregulatory system. Am J Physiol Regul Integr Comp Physiol 292:R37–R46.

Romanovsky AA, Ivanov AI, Shimansky YP (2002) Ambient temperature for experiments in rats: a new method for determining the zone of thermal neutrality. J Appl Physiol 92:2667–2679.

Romanovsky AA, Sugimoto N, Simons CT, Hunter WS (2003) The *organum vasculosum laminae terminalis* in immune-to-brain febrigenic signaling: a reappraisal of lesion experiments. Am J Physiol Regul Integr Comp Physiol 285:R420–R428.

Rudaya AY, Steiner AA, Robbins JR, Dragic AS, Romanovsky AA (2005) Thermoregulatory responses to lipopolysaccharide in the mouse: dependence on the dose and ambient temperature. Am J Physiol Regul Integr Comp Physiol 289:R1244–R1252.

Sakaguchi T, Yamazaki M (1988) Hepatic portal injection of glucose elevates efferent sympathetic discharges of interscapular brown adipose tissue. Exp Neurol 101:464–469.

Sanchez JF, Krause JE, Cortright DN (2001) The distribution and regulation of vanilloid receptor VR1 and VR1 5′ splice variant RNA expression in rat. Neuroscience 107:373–381.

Schicho R, Florian W, Liebmann I, Holzer P, Lippe IT (2004) Increased expression of TRPV1 receptor in dorsal root ganglia by acid insult of the rat gastric mucosa. Eur J Neurosci 19:1811–1818.

Shimizu I, Iida T, Horiuchi N, Caterina MJ (2005) 5-iodoresiniferatoxin evokes hypothermia in mice and is a partial transient receptor potential vanilloid 1 agonist *in vitro*. J Pharmacol Exp Ther 314:1378–1385.

Steiner AA, Rudaya AY, Ivanov AI, Romanovsky AA (2004) Febrigenic signaling to the brain does not involve nitric oxide. Br J Pharmacol 141:1204–1213.

Swanson DM, Dubin AE, Shah C, Nasser N, Chang L, Dax SL, Jetter M, Breitenbucher JG, Liu C, Mazur C, Lord B, Gonzales L, Hoey K, Rizzolio M, Bogenstaetter M, Codd EE, Lee DH, Zhang SP, Chaplan SR, Carruthers NI (2005) Identification and biological evaluation of 4-(3-trifluoromethylpyridin-2-yl)piperazine-1-carboxylic acid (5-trifluoromethylpyridin-2-yl)amide, a high affinity TRPV1 (VR1) vanilloid receptor antagonist. J Med Chem 48:1857–1872.

Szelenyi Z, Szekely M, Romanovskii AA (1992) The central thermoregulatory action of cholecystokinin-8 and prostaglandin E_1 (in Russian). Fiziol Zh SSSR Im I M Sechenova 78:94–101.

Szelenyi Z, Hummel Z, Szolcsanyi J, Davis JB (2004) Daily body temperature rhythm and heat tolerance in TRPV1 knockout and capsaicin pretreated mice. Eur J Neurosci 19:1421–1424.

Tominaga M, Caterina MJ (2004) Thermosensation and pain. J Neurobiol 61:3–12.

Tominaga M, Caterina MJ, Malmberg AB, Rosen TA, Gilbert H, Skinner K, Raumann BE, Basbaum AI, Julius D (1998) The cloned capsaicin receptor integrates multiple pain-producing stimuli. Neuron 21:531–543.

Woods AJ, Stock MJ, Gupta AN, Wong TT, Andrews PL (1994) Thermoregulatory effects of resiniferatoxin in the rat. Eur J Pharmacol 264:125–133.

Zhang L, Jones S, Brody K, Costa M, Brookes SJ (2004) Thermosensitive transient receptor potential channels in vagal afferent neurons of the mouse. Am J Physiol Gastrointest Liver Physiol 286:G983–G991.

Zygmunt PM, Petersson J, Andersson DA, Chuang H, Sorgard M, Di Marzo V, Julius D, Hogestatt ED (1999) Vanilloid receptors on sensory nerves mediate the vasodilator action of anandamide. Nature 400:452–457.

Supplemental Materials and Methods

Synthesis of AMG0347

Step 1. Piperidine (800 mmol) was added to a solution of 2-chloro-6-(trifluoromethyl)nicotinic acid (89 mmol) in *N,N*-dimethylformamide (80 ml). The mixture was stirred at room temperature under nitrogen for 20 h and then acidified with 5 M HCl to a final pH of 3.0. The reaction products were extracted with ethyl acetate (3 × 100 ml). The ethyl acetate phase was washed with water and brine, dehydrated with magnesium sulfate, and concentrated *in vacuo*. The concentrated phase contained 84 mmol (95% reaction yield) of 2-(piperidin-1-yl)-6-(trifluoromethyl) nicotinic acid [*intermediary 1*; MS (ESI, positive ion) m/z: 274.8 (M+1)].

Step 2. Lithium aluminum hydride (84 mmol) was added to a cold (0ºC) solution of *intermediary 1* (84 mmol) in tetrahydrofurane (200 ml). After the mixture was allowed to react at room temperature under constant stirring for 20 h, more lithium aluminum hydride was added as a 20 ml aliquot of a 1 M solution in tetrahydrofurane, and the reaction was allowed to continue for additional 6 h. The reaction was quenched by a dropwise addition of water (10 ml) and potassium hydroxide (30 ml of a 20% solution in water). The quenched reaction mixture was stirred for 1 h, filtered, and the filtrate was evaporated *in vacuo*. The residue obtained was suspended in water (100 ml), and the pH of this solution was adjusted to 7.0 with 2 N HCl. The reaction product was then extracted with ethyl acetate (4 × 100 ml). As before, the ethyl acetate phase was washed with water and brine, treated with magnesium sulfate, and concentrated *in vacuo*. The crude product was purified using silica gel column chromatography (mobile phase: ethyl acetate-hexanes, 1:9). At the end of this step, we obtained 53.9 mmol (64% reaction yield) of (2-(piperidin-1-yl)-6-(trifluoromethyl)pyridin-3-yl)methanol [*intermediary 2*; ^{1}H NMR (300 MHz, CDCl$_3$): δ 1.59-1.69 (m, 2H), 1.69-1.81 (m, 4H), 3.06-3.20 (m, 4 H), 3.85 (s, 1H), 4.78 (s, 2H), 7.32 (d, J = 7.72 Hz, 1H), 7.74 (d, J = 8.29 Hz, 1H)].

Step 3. Manganese dioxide (260 mmol) was added to 100 ml of dicholoromethane containing *intermediary 2* (52.0 mmol). The mixture was allowed to react under constant stirring for 1 h and then filtered. The residue obtained after *in-vacuo* evaporation of the solvent contained 46 mmol (90% reaction yield) of 2-(piperidin-1-yl)-6-(trifluoromethyl)-nicotinaldehyde [*intermediary 3*; MS (ESI, postive ion) m/z: 259.1 (M+1); ^{1}H NMR (300 MHz, CDCl$_3$): δ 1.72 (s, 6 H), 3.52 (s, 4H), 7.15 (d, J = 7.72 Hz, 1H), 8.09 (d, J = 7.72 Hz, 1H), 9.99 (s, 1H)].

Step 4. A solution consisting of triethylphosphono acetate (56 mmol), lithium chloride (46 mmol), N-ethyl-N-isopropylpropan-2-amine (46 mmol), and acetonitrile (40 ml) was stirred for 20 min at room temperature, and then mixed with a solution of *intermediary 3* (46 mmol) in acetonitrile (80 ml). The mixture was stirred at room temperature for 20 h under nitrogen. The solvents were evaporated *in vacuo*, and the residue was partitioned between ethyl acetate and water. The aqueous phase was extracted with ethyl acetate (4 × 100 ml). As before, the ethyl acetate phase was washed with water and brine, treated with magnesium sulfate, and concentrated *in vacuo*. The crude product was purified by silica gel column chromatography (hexanes-acetone, 9:1). The purified product consisted of 41.1 mmol (88% reaction yield) of (*E*)-ethyl3-(2-(piperidin-1-yl)-6-(trifluoro-methyl)-pyridin-3-yl)acrylate [*intermediary 4*; MS (ESI, postive ion) m/z: 328.9 (M+1); ^{1}H NMR (300 MHz, CDCl$_3$): δ 1.36 (t, J = 7.16 Hz, 3H), 1.73 (d, J = 3.39 Hz, 6H), 3.24-3.35 (m, 4H), 4.29 (q, J = 7.16 Hz, 2 H), 6.43 (d, J = 16.01 Hz, 1H), 7.17 (d, J = 7.54 Hz, 1H), 7.70 (d, J = 16.20 Hz, 1H), 7.77 (d, J = 7.72 Hz, 1H)].

Step 5. Potassium hydroxide (100 ml of a 1.23 M solution in water) was then added to a solution of *intermediary 4* (41.1 mmol) in dioxane (100 ml). Under nitrogen, the resulting mixture was first heated to reflux for 4 h and then allowed to cool to room temperature. The solvents were evaporated *in vacuo*, and the residue was partitioned between ethyl acetate and water. HCl (2 M) was used to acidify (pH = 3) the aqueous phase, which was then subjected to extraction with ethyl acetate (4 × 100 ml). Once more, the ethyl acetate phase was washed with water and brine, treated with magnesium sulfate, and concentrated *in vacuo*. The crude product was purified by silica gel column chromatography (9:1 hexanes-ethyl acetate followed by 80:18:2 hexanes-ethyl acetate-acetic acid). At the end of this step, we obtained 36.7 nmol (91% reaction yield) of (*E*)-3-(2-(piperidin-1-yl)-6-(trifluoromethyl)pyridin-3-yl) acrylic acid [*intermediary 5*; MS (ESI, postive ion) m/z: 300.9 (M+1); ^{1}H NMR (300 MHz, CDCl$_3$): δ 1.63-1.81 (m, 6H), 3.27-3.36 (m, 4H), 6.44 (d, J = 16.01 Hz, 1H), 7.18 (d, J = 7.72 Hz, 1H), 7.79 (d, J = 16.01 Hz, 1H), 7.81 (d, J = 7.72 Hz, 1H)].

Step 6. To a solution of *intermediary 5* (18 mmol) in *N,N*-dimethylformamide (50 ml) were added 8-amino-1,2,3,4-tetrahydronaphthalen-2-ol (27 mmol), 1H-benzo[d][1,2,3]triazol-1-ol (27 mmol), *N*1-((ethyliminomethylene)-*N*3,*N*3-dimethylpropane-1,3-diamine hydrochloride (20 mmol), and *N*-ethyl-*N*-isopropylpropan-2-amine (37 mmol). The mixture was stirred at room temperature under nitrogen for 20 h. The reaction mixture was partitioned between ethyl acetate and a saturated aqueous solution of sodium bicarbonate, after which the aqueous phase was extracted with ethyl acetate (2 x 100 ml). The ethyl acetate phase was washed with brine, dried over magnesium sulfate, and the solvents were removed *in vacuo*. The crude product was purified by silica gel column chromatography (hexanes-ethyl acetate, 4:1). The purified product was a yellow solid that consisted of 11.9 mmol (65% reaction yield) of (*E*)- N -(7-hydroxy-5,6,7,8-tetrahydronaphthalen-1-yl)- 3 -(2-(piperidin- 1-yl)-6-(trifluoromethyl)pyridin-3-yl) acrylamide [*AMG0347*; MS (ESI, positive ion) m/z: 445.8 (M+1); ^{1}H NMR (300 MHz, CDCl$_3$): δ 1.60-1.77 (m, 6H), 1.80 (d, J = 4.52 Hz, 2H), 2.00-2.15 (m, 1 H), 2.61 (dd, J = 16.11, 7.63 Hz, 1 H), 2.76-2.94 (m, 1 H), 2.94-3.09 (m, 2 H), 3.32 (s, 4H), 4.21 (d, J = 4.14 Hz, 1H), 6.58 (d, J = 15.64 Hz, 1H), 7.01 (d, J = 7.16 Hz, 1H), 7.08-7.24 (m, 3H), 7.78 (d, J = 15.45 Hz, 2H), 7.76-7.80 (m, 1H); combustion analysis: C = 64.48, H = 5.84, N = 9.43 (these values matched well the expected values of 64.71, 5.88, and 9.43, respectively)].
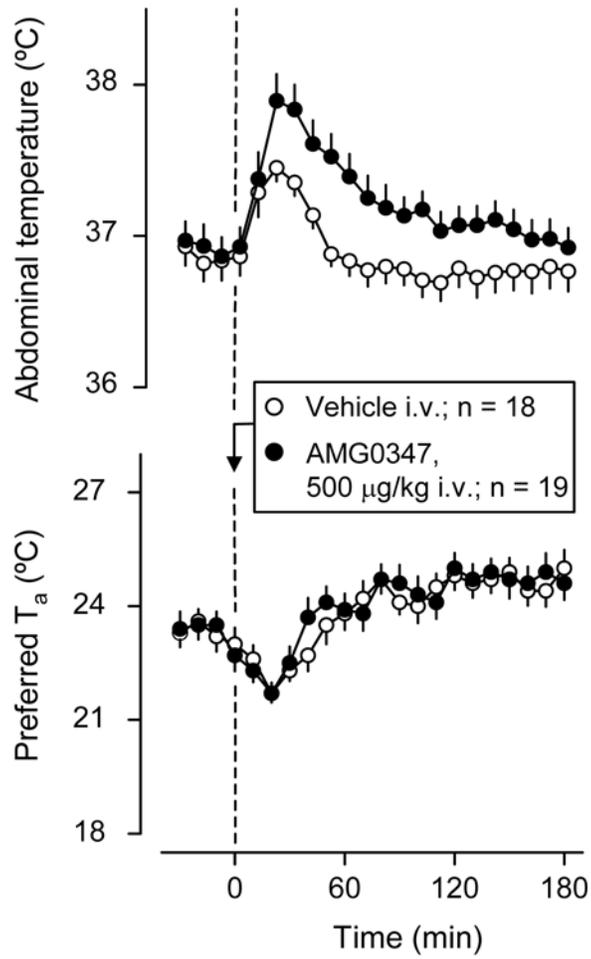
Supplemental Figure 1. AMG0347 does not affect thermal preference. The effects of AMG0347 and its vehicle on the abdominal temperature and preferred T_a of rats in a thermogradient apparatus are shown.
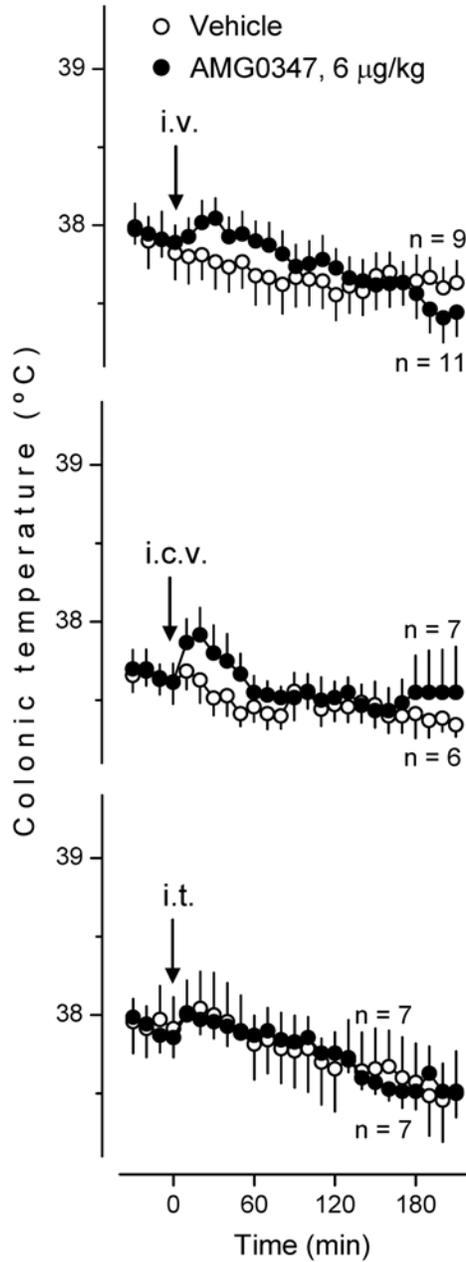
Supplemental Figure 2. When administered directly into the brain or spinal cord, AMG0347 is no more effective in causing hyperthermia than when administered systemically. The figure shows the colonic temperature of rats administered with a low dose of AMG0347 (or with its vehicle) via the intravenous (i.v.), intracerebroventricular (i.c.v.), or intrathecal (i.t.) route at thermoneutrality (T_a of 24ºC).